

Graphene-based fiber polarizer with PVB-enhanced light interaction

Haojie Zhang, Noel Healy, Li Shen, Chung Che Huang, Nikos Aspiotis, Dan W. Hewak, and Anna C. Peacock

Abstract—Graphene is a two-dimensional material which, as a result of its excellent photonic properties, has been investigated for a wide range of optical applications. In this paper, we propose and fabricate a commercial grade broadband graphene-based fiber polarizer using a low loss side-polished optical fiber platform. A high index polyvinyl butyral layer is used to enhance the light-graphene interaction of the evanescent field of the core guided mode to simultaneously obtain a high extinction ratio ~ 37.5 dB with a low device loss ~ 1 dB. Characterization of the optical properties reveals that the polarizer retains low transmission losses and high extinction ratios across an extended telecoms band. The results demonstrate that side-polished fibers are a useful platform for leveraging the unique properties of low-dimensional materials in a robust and compact device geometry.

Index Terms—Graphene, polarizer, side-polished fiber, extinction ratio, transmission loss.

I. INTRODUCTION

Optical polarizers and polarization devices are integral components in both optical communications systems and polarization-dependent optical sensors. Conventional polarizers typically use bulk optical configurations which are difficult to align and interface with fiber networks [1]. Thus efficient, low loss, all-fiber-based polarization components are highly desirable for seamless integration within existing systems. One method of constructing a fiber polarizer is to use an optical fiber with a portion of its cladding removed and replaced with a thin-film overlay. Materials that have been used for this purpose include metal films [2], birefringent crystals [3] and liquid crystals [4]. However, these devices typically have a relatively narrow operation bandwidth, and/or high losses, which limit their application potential.

In terms of extending the operation bandwidth, graphene is an excellent choice of material as its linear and gapless band dispersion result in flat, broadband absorption and high quantum efficiency [5]. Owing to these desirable optoelectronic properties, graphene has been considered for a wide array of optical devices, such as all-optical modulators [6], Q-switched or mode-locked ultrafast lasers [7], [8], nonlinear processing [9], and ultra-broadband photodetectors [10]. Of particular

H. Zhang, L. Shen, C. C. Huang, N. Aspiotis and A. C. Peacock are with the Optoelectronics Research Centre, University of Southampton, Southampton, SO17 1BJ, U.K. (e-mail: hz15e13@soton.ac.uk; ls1q11@soton.ac.uk; cch@soton.ac.uk; nka1q14@soton.ac.uk; dh@soton.ac.uk; acp@orc.soton.ac.uk).

Noel Healy was with the Optoelectronics Research Centre, University of Southampton, Southampton, SO17 1BJ, U.K. and is currently with the Emerging Technology and Materials Group, School of Electrical and Electronic Engineering, Newcastle University, Newcastle upon Tyne, NE1 7RU, UK. (e-mail: noel.healy@ncl.ac.uk).

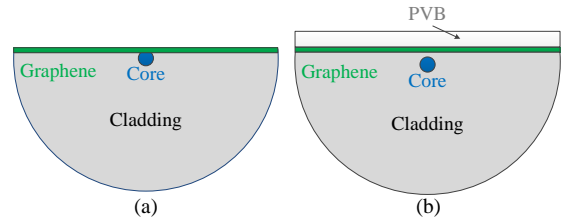


Fig. 1: (a) Cross-section of a graphene-based fiber polarizer with side-polishing into the fiber core, as per [11]. (b) Cross-section of the fiber polarizer used in this study with a residual cladding between the core and the graphene layer.

relevance to our work, several graphene-based optical polarizers have already been proposed and demonstrated [11]–[13], including one device based on a side-polished optical fiber, as shown in Fig. 1(a) [11]. However, for this particular configuration, in order to achieve a material interaction sufficient for an extinction ratio of 19 dB, the graphene was placed in contact with the core, resulting in impractically high losses (~ 20 dB at 1550 nm). Other devices such as the planar waveguide-based graphene polarizer proposed in [13], have also exhibited large losses, in this case ~ 20 dB at 1310 nm [13]. These results make it obvious that an alternative approach is required to obtain both the high performance and low device losses required for fiber-based systems.

In this paper, we present a novel approach to producing a low loss, high extinction ratio graphene-based polarizer. The device is based on a modified side-polished fiber design together with a graphene/polymer heterostructure that enhances the light-graphene interaction. The polarizer has an extinction ratio of ~ 37.5 dB at 1550 nm for a loss of ~ 1 dB. To our knowledge, this device offers an order of magnitude improvement in performance over any previously reported fiber-based graphene polarizers, while at the same time reducing the device loss by more than two orders of magnitude. The experimental results are in good agreement with the numerical investigations, which highlight the usefulness of these side-polished fibers as templates for the integration of other low-dimensional materials.

II. DEVICE DESIGN

Side-polished optical fibers present a unique opportunity to study the interaction of light and matter in a configuration where the path of the propagating light is unbroken. As such, the platform has many key benefits such as robustness, long interaction lengths and controllable interaction strengths. The

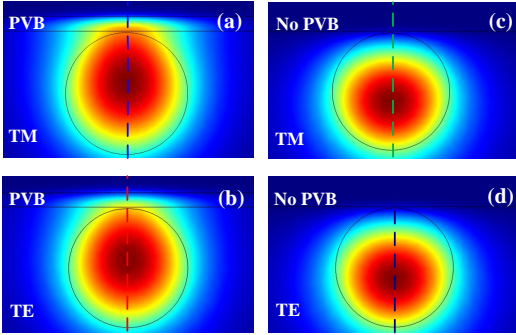


Fig. 2: Numerical finite element simulations of modes within the uniform polished sections at 1550 nm. Electric field distributions for (a) TM and (b) TE modes of a side-polished optical fiber with PVB-coated graphene layer, and for (c) TM and (d) TE modes of the same fiber but with graphene only at the polished surface.

approach developed in this paper is based on a side-polished fiber where the interaction window is polished close to, but not into the core, thus suppressing the transmission losses. However, a drawback of this design is that the field of the core guided mode will be very low at the surface of the window, resulting in a weak interaction with the mono-layer graphene film. To address this issue, we introduce a high index polyvinyl butyral (PVB) over-layer, which helps to draw out the evanescent tail of the propagating core mode and enhance the light-graphene interaction. The longitudinal cross-section of the device is illustrated in Fig. 1(b), which clearly shows the three-layer structure. Importantly, as PVB exhibits low optical losses over most of the transmission window of the silica fiber platform, with appropriate design these multi-layer devices could be made to operate from visible wavelengths up to the edge of the mid-infrared.

The absorption of graphene arises from the material’s intraband and interband transitions, and either can dominate depending on the chemical potential [14]. In our work, we make use of mono-layer graphene prepared by the CVD method, which is estimated to have a chemical potential on the order of 0.1 eV [15]. Previous work has shown that for potentials of this value, the conductivity of the graphene sheet has a large negative imaginary component [16], so that the interband transition dominates the absorption. Thus we expect the TM mode of the fiber to be preferentially absorbed by the graphene sheet, resulting in a TE-pass polarizer [11].

In order to determine the effect that the PVB layer has on the transmission properties of the device, a numerical finite element study was undertaken. As a starting point, the operation wavelength was set at 1550 nm where the corresponding refractive index of PVB ($n_g = 1.48$) is slightly larger than that of the silica fiber ($n_s = 1.45$). Fig. 2(a) and (b) show the electromagnetic field distributions of the fundamental TM and TE modes at the uniform polished sections of the fiber when coated with a 1 μm thick PVB layer on top of the graphene. For comparison, Fig. 2(c) and (d) show the same modes calculated without the PVB layer. These figures clearly illustrate the increased light-matter interaction at the polished

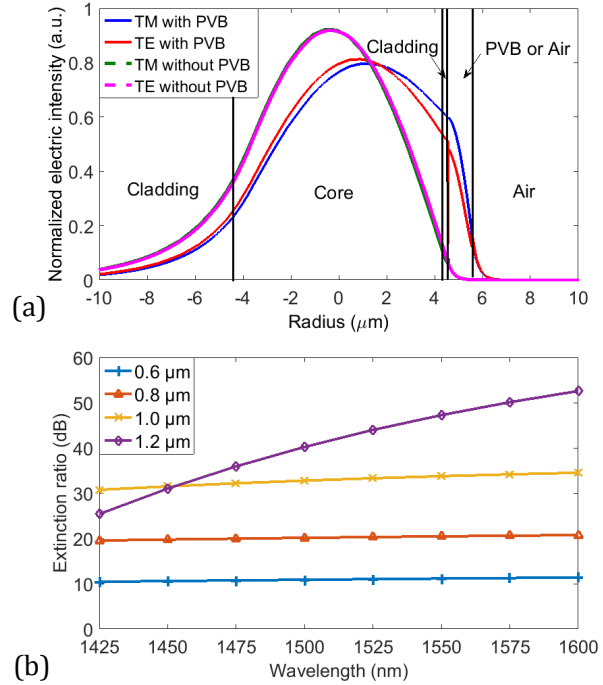


Fig. 3: (a) Normalized cross-sectional line scan along dashed lines indicated in Fig. 2. (b) Numerical simulation results showing the extinction ratio as a function of wavelength for different thicknesses of the PVB layer.

fiber surface when the high index layer is included. Further verification is provided by Fig. 3(a), which shows the intensity distribution across the positions indicated by the dashed lines in Fig. 2. From this figure, we estimate an increase of ~ 10 dB of modal interaction at the polished surface, which can be attributed to the PVB over-layer. To investigate the influence the layer thickness has on this interaction, Fig. 3(b) plots the calculated extinction ratio as a function of wavelength when the PVB thickness varies from 0.6 μm to 1.2 μm in 0.2 μm steps. In general, a thicker PVB layer results in a larger extinction ratio across the wavelength range shown here. However, when the thickness reaches a value of 1.2 μm , the core guided mode becomes leaky for both polarizations. This effect is more distinct at shorter wavelengths and results in a large reduction of extinction ratio. Thus a 1 μm thick PVB layer was deemed to be the optimum choice for this work.

III. FABRICATION AND EXPERIMENT

To fabricate the side-polished fibers, a modified block polishing technique was used to remove a portion of the cladding from a standard single mode fiber (SMF). The fiber was polished until the planar surface was formed at a distance of $\sim 1 \mu\text{m}$ from the core. The roughness of the polished surface was measured via a Ze-scope profilometer to be as low as 1 nm RMS and an adiabatic transition from the fiber’s full circular geometry to the D-shaped uniform polished region was maintained, resulting in a polished fiber with negligible transmission loss [17]. Fig. 4(a) shows a SEM image of the top surface of the side-polished fiber, providing evidence of its ultra smooth surface. The polished region permitted access

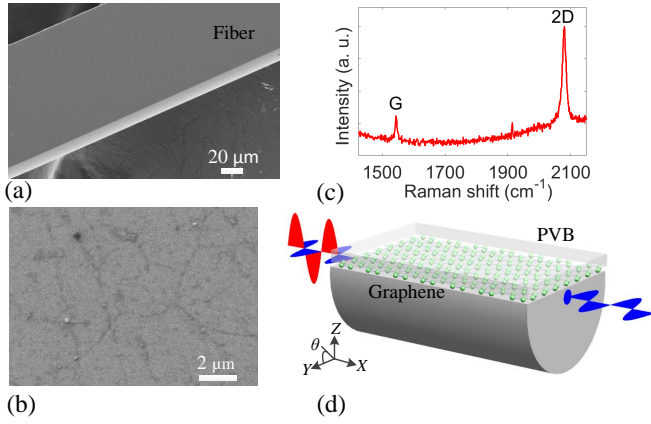


Fig. 4: (a) SEM image of our side-polished fiber. (b) Helium-ion microscope image of the graphene sheet and (c) the corresponding Raman spectrum. (d) Schematic model of the PVB-coated graphene polarizer based on a side-polished optical fiber. Polarization angle θ is defined as $\theta = 0^\circ$ and 180° for TE mode (blue light wave), $\theta = 90^\circ$ and 270° for TM mode (red light wave).

to more than 30 dB of the light propagating through the core. This was verified by dropping a high refractive index liquid onto the polished region and monitoring the change in transmitted power.

The mono-layer graphene film was grown on a copper substrate by a chemical vapor deposition (CVD) method. Fig. 4(b) displays a helium-ion microscope image of the CVD grown graphene sheet, which clearly shows its high quality and uniform thickness. Further confirmation of the monolayer nature is provided by the Raman spectrum in Fig. 4(c), where the narrow 2D peak (25 cm^{-1} FWHM) is more than 4 times stronger than the G peak [18]. A $1 \mu\text{m}$ -thick PVB layer was subsequently spin coated directly onto the bare graphene surface and baked for 5 minutes at 85°C . The copper substrate was etched away in an ammonium persulfate solution, leaving only the PVB-coated graphene sheet. The sheet was then rinsed in DI water, before being transferred onto the polished fiber’s planar surface. Finally, the fiber was baked at 60°C for 10 minutes to thoroughly evaporate the water and improve the contact between the graphene film and the fiber. A schematic

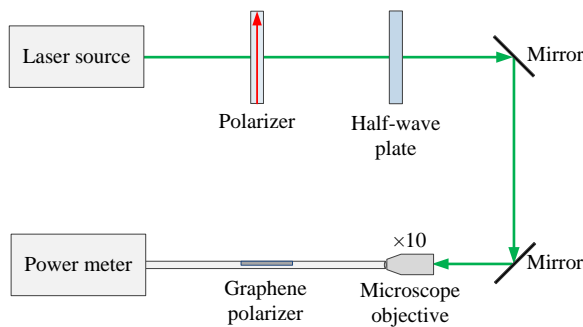


Fig. 5: Experimental configuration of the polarization measurements excited by near-infrared light.

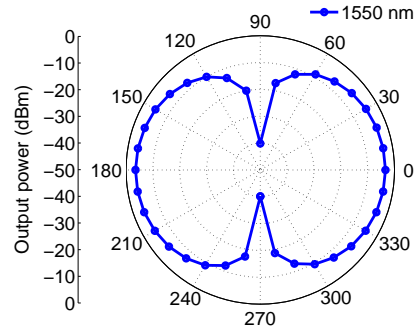


Fig. 6: Polar plot of the output power measured at 1550 nm when input power is 0 dBm.

view of the resulting device is presented in Fig. 4(d).

To characterize the optical transmission properties of the PVB-coated graphene-based fiber polarizer, the experimental configuration presented in Fig. 5 was used. A tunable continuous wave (CW) laser (1425 to 1600 nm) was chosen for the signal so that the optical properties could be measured across a broad wavelength range. The signal was free-space coupled into the device using a $10\times$ magnification microscope objective lens. Prior to this, polarization control was used to ensure the fidelity of the linear polarization state. The half-wave plate could then be used to rotate the polarization of the input light. Since standard SMF fibers are used in this study, the fiber lengths were kept short and the device was maintained as straight as possible to prevent unwanted polarization rotation. The output power was then monitored via a power meter for different polarization angles and wavelengths.

An example polar plot of the transmitted power as a function of polarization angle is shown in Fig. 6, for the wavelength of 1550 nm. It is clear that for the angles of 0° and 180° , when the TE mode was aligned to interact with the graphene, the transmission was maximized and when the polarization was rotated to 90° and 270° the transmission dropped by 37.5 dB, evidence of the TE pass nature of our device. To determine the magnitude of enhancement of the light-graphene interaction due to the PVB, the experiment was repeated on a device with a graphene only layer. In this experiment the

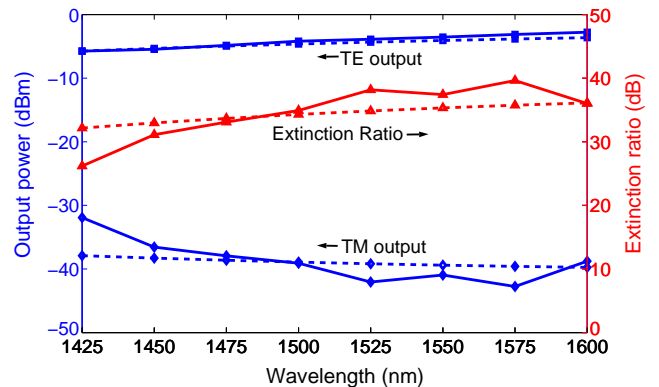


Fig. 7: Solid lines: experimental output powers for TE & TM modes and corresponding extinction ratios. Dash lines: predicted extinctions obtained from simulations in Section II.

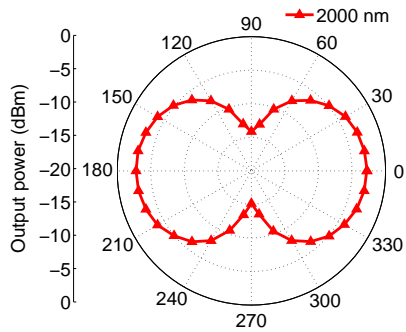


Fig. 8: Polar plot of the output power measured at 2000 nm when input power is 0 dBm.

extinction ratio was just 3 dB, thus the PVB layer increased the interaction by more than 30 dB in agreement with Fig. 3(a). A control experiment was also performed on a bare side-polished fiber to determine the extent of the polarizing effect of the D-shaped structure. When polished to a distance of 1 μm from the core, the bare fiber showed no evidence of any polarization dependent attenuation.

Additional polarization measurements were also undertaken across the full wavelength range of our tunable laser source (1425 to 1600 nm) and at each wavelength, the extinction ratio did not drop below 26 dB (Fig. 7). These results also agree well with the theoretical simulation results calculated over this range (dash lines in Fig. 7), providing clear evidence of the broadband nature of our device and the significant improvement in the performance over previously reported results [11]–[13]. Moreover, the polarization extinction ratio increases with larger incident wavelengths. This is because absorption of the TM light increases with increasing wavelength, which can be explained by the higher evanescent field of the longer wavelengths at the graphene interface.

To provide further evidence of the broadband nature of the device, the measurements were extended to a operating wavelength of 2000 nm using a laser diode. The polar plot in Fig. 8 shows the result of this experiment with a maximum value of -3.5 dB and a minimum of -16.5 dB detected at the output of our device. Comparing this to the results at 1550 nm, we attribute the lower extinction ratio of 13 dB to the limited polarization maintenance of the standard SMF fiber at this longer wavelength. Nevertheless, these results represent the highest extinction ratio measured at 2000 nm for a graphene-based fiber polarizer. Finally, it is also worth noting that as well as enhancing the light-graphene interaction, the PVB film also acts as a protective over-layer to improve the long-term stability of these devices, and no degradation has been observed when monitoring their performance over a 12-month period.

IV. CONCLUSION

In conclusion, we have designed and experimentally demonstrated a graphene-based fiber polarizer with a high extinction ratio of ~ 37.5 dB and a low device loss of ~ 1 dB. Furthermore, an extinction ratio greater than 26 dB was recorded across the wavelength range 1425 – 1600 nm, with

an additional value of 13 dB at 2000 nm, which confirms the broadband nature of our device. As the reduced extinction at 2000 nm is most likely due to the limited polarization maintenance of the SMF at this wavelength, we expect that more optimal fiber designs will enable device operation across the fibre's entire single-mode transmission window. We believe that, owing to the combination of low losses and high extinction ratios, this device is the first truly practical graphene-fiber device for photonics applications. This simple and effective scheme for enhanced light-matter interaction could easily be adapted for other two-dimensional materials such as MoS_2 or black phosphors [19], thus serving as a platform for a new generation of all-fiber optoelectronic devices.

ACKNOWLEDGMENT

H. Zhang thanks the China Scholarship Council for funding. The authors acknowledge EPSRC for financial support through EP/J004863/1 and the Centre for Innovative Manufacturing in Photonics (EP/H02607X/1). They also thank Jamie Reynolds for the Helium-ion microscope image.

REFERENCES

- [1] D. H. Goldstein, *Polarized light*. CRC Press, 2010.
- [2] J. Feth and C. Chang, "Metal-clad fiber-optic cutoff polarizer," *Opt. Lett.*, vol. 11, no. 6, pp. 386–388, 1986.
- [3] R. A. Bergh, H. C. Lefevre, and H. J. Shaw, "Single-mode fiber-optic polarizer," *Opt. Lett.*, vol. 5, no. 11, pp. 479–481, 1980.
- [4] K. Liu, W. Sorin, and H. Shaw, "Single-mode-fiber evanescent polarizer/amplitude modulator using liquid crystals," *Opt. Lett.*, vol. 11, no. 3, pp. 180–182, 1986.
- [5] S. Zhou, G.-H. Gweon, J. Graf, A. Fedorov, C. Spataru, R. Diehl, Y. Kopelevich, D.-H. Lee, S. G. Louie, and A. Lanzara, "First direct observation of dirac fermions in graphite," *Nature Phys.*, vol. 2, no. 9, pp. 595–599, 2006.
- [6] M. Liu, X. Yin, E. Ulin-Avila, B. Geng, T. Zentgraf, L. Ju, F. Wang, and X. Zhang, "A graphene-based broadband optical modulator," *Nature*, vol. 474, no. 7349, pp. 64–67, 2011.
- [7] D. Popa, Z. Sun, T. Hasan, F. Torrisi, F. Wang, and A. Ferrari, "Graphene q-switched, tunable fiber laser," *Appl. Phys. Lett.*, vol. 98, no. 7, p. 3106, 2011.
- [8] H. Zhang, D. Tang, L. Zhao, Q. Bao, and K. Loh, "Large energy mode locking of an erbium-doped fiber laser with atomic layer graphene," *Opt. Express*, vol. 17, no. 20, pp. 17630–17635, 2009.
- [9] H. Zhang, S. Virally, Q. Bao, L. K. Ping, S. Massar, N. Godbout, and P. Kockaert, "Z-scan measurement of the nonlinear refractive index of graphene," *Opt. Lett.*, vol. 37, no. 11, pp. 1856–1858, 2012.
- [10] F. Xia, T. Mueller, R. Golizadeh-Mojarad, M. Freitag, Y.-m. Lin, J. Tsang, V. Perebeinos, and P. Avouris, "Photocurrent imaging and efficient photon detection in a graphene transistor," *Nano Lett.*, vol. 9, no. 3, pp. 1039–1044, 2009.
- [11] Q. Bao, H. Zhang, B. Wang, Z. Ni, C. H. Y. X. Lim, Y. Wang, D. Y. Tang, and K. P. Loh, "Broadband graphene polarizer," *Nature Photon.*, vol. 5, no. 7, pp. 411–415, 2011.
- [12] Y. V. Bludov, M. I. Vasilevskiy, and N. M. Peres, "Tunable graphene-based polarizer," *J. Appl. Phys.*, vol. 112, no. 8, p. 084320, 2012.
- [13] J. T. Kim and C.-G. Choi, "Graphene-based polymer waveguide polarizer," *Opt. Express*, vol. 20, no. 4, pp. 3556–3562, 2012.
- [14] J. Gosciniaik and D. T. Tan, "Theoretical investigation of graphene-based photonic modulators," *Sci. Rep.*, vol. 3, p. 1897, 2013.
- [15] J. Horng, C.-F. Chen, B. Geng, C. Girit, Y. Zhang, Z. Hao, H. A. Bechtel, M. Martin, A. Zettl, M. F. Crommie, *et al.*, "Drude conductivity of dirac fermions in graphene," *Phys. Rev. B*, vol. 83, no. 16, p. 165113, 2011.
- [16] K. F. Mak, M. Y. Sfeir, Y. Wu, C. H. Lui, J. A. Misewich, and T. F. Heinz, "Measurement of the optical conductivity of graphene," *Phys. Rev. Lett.*, vol. 101, no. 19, p. 196405, 2008.
- [17] H. Zhang, N. Healy, L. Shen, C. C. Huang, D. W. Hewak, and A. C. Peacock, "Enhanced all-optical modulation in a graphene-coated fibre with low insertion loss," *Sci. Rep.*, vol. 6, p. 23512, 2016.

- [18] A. Ferrari, J. Meyer, V. Scardaci, C. Casiraghi, M. Lazzeri, F. Mauri, S. Piscanec, D. Jiang, K. Novoselov, S. Roth, *et al.*, "Raman spectrum of graphene and graphene layers," *Phys. Rev. Lett.*, vol. 97, no. 18, p. 187401, 2006.
- [19] S. Lu, L. Miao, Z. Guo, X. Qi, C. Zhao, H. Zhang, S. Wen, D. Tang, and D. Fan, "Broadband nonlinear optical response in multi-layer black phosphorus: an emerging infrared and mid-infrared optical material," *Opt. Express*, vol. 23, no. 9, pp. 11183–11194, 2015.